Ahmet Kursat Karaman[1]
Bora Korkmazer[2]
Enise Yagmur Ozkan[3]
Enes Değer[3]
Cihan Isler[4]
Cesur Samanci[3]
Ahmet Bas[3]
Rugiyya Ahmadli[5]
Serdar Arslan[2]
Osman Kizilkilic[2]

[1] Department of Radiology, Sureyyapasa Chest Diseases and Thoracic Surgery Training Hospital, Istanbul, Türkiye
[2] Division of Neuroradiology, Department of Radiology, Istanbul University-Cerrahpasa, Istanbul, Türkiye
[3] Department of Radiology, Istanbul University-Cerrahpasa, Istanbul, Türkiye
[4] Department of Neurosurgery, Istanbul University-Cerrahpasa, Istanbul, Türkiye
[5] Department of Radiology, Azerbaijan Medical University, Baku, Azerbaijan

Corresponding Author:
Ahmet Kursat Karaman
mail:kursat.karaman@istanbul.edu.tr

Conventional and Diffusion MR Imaging Features of Ring-shaped Lateral Ventricular Nodules

ABSTRACT

Objective: The aim of this study is to evaluate the conventional and diffusion MRI findings of ring-shaped lateral ventricular nodules (RSLVN) along with clinical features.

Materials and Methods: MR images of all patients who underwent contrast-enhanced brain MRI between 2019 and 2023 were retrospectively evaluated. The number, shape, maximal diameter, and signal intensity of RSLVNs on T1-weighted (T1W), T2-weighted (T2W), fluid-attenuated inversion recovery (FLAIR) and diffusion-weighted imaging (DWI), and contrast-enhancement status were evaluated. Apparent diffusion coefficient (ADC) values and normalized ADC ratios of nodules were also determined. If follow-up MRIs were performed, morphological changes of RSLVNs were evaluated.

Results: RSLVN was observed in fifteen (0.51%) of 2920 patients. Multiple RSLVNs were observed in five patients and therefore a total of 23 RSLVNs were identified in fifteen patients. Nodules were located on the roof of the lateral ventricle in eight nodules (34.8%), in the frontal horn in twelve nodules (52.2%), and in the septum pellucidum in three. 6 of 23 RSLVNs (26.1%) were larger than 1 cm. All RSLVNs were isointense on T1W and T2W, while hyperintense on FLAIR. On DWI, 20 of 23 RSLVNs had isointense signal and the remaining 3 lesions were hyperintense. The mean ADC value and nADC ratio were $1.42 \pm 0.29 \times 10^{-3} mm^2$ and 1.87 ± 0.31, respectively.

Conclusions: RSLVNs may be more frequent than previously reported. Their uniform MRI appearance and typical localizations are distinctive, and they can reach relatively large sizes. Morphological stability during follow-up and the ADC values of these lesions suggest a possible benign nature.

Keywords: RSLVN, Neuroimaging, Magnetic Resonance Imaging, Nodule, Lateral Ventricle.

Halka Şekilli Lateral Ventrikül Nodüllerinin Konvansiyonel ve Diffüzyon MR Görüntüleme Özellikleri

ÖZET

Amaç: Bu çalışmanın amacı halka şekilli lateral ventrikül nodüllerinin (RSLVN) konvansiyonel ve difüzyon MR bulgularını klinik özellikleriyle birlikte değerlendirmektir.

Gereç ve Yöntem: 2019-2023 yılları arasında kontrastlı beyin MR çekimi bulunan tüm hastaların MR görüntüleri retrospektif olarak değerlendirildi. T1 ağırlıklı (T1W), T2 ağırlıklı (T2W), FLAIR ve difüzyon ağırlıklı görüntülemede (DAG) RSLVN'lerin sayısı, şekli, maksimum çapı ve sinyal yoğunluğu ve kontrast tutulum durumu değerlendirildi. Nodüllerin görünür difüzyon katsayısı (ADC) değerleri ve normalleştirilmiş ADC oranları da belirlendi. Takip MR'ları yapıldıysa, RSLVN'lerin zaman içerisindeki morfolojik değişiklikleri değerlendirildi.

Bulgular: Çalışmaya dahil edilen 2920 hastanın 15'inde (%0,51) RSLVN saptandı. Beş hastada birden fazla RSLVN gözlendi ve dolayısıyla on beş hastada toplam 23 RSLVN tanımlandı. Nodüllerin sekizi (%34,8) lateral ventrikül tavanında, on iki tanesi (%52,2) ön boynuzda, üçü ise septum pellucidum'da yerleşmişti. 23 RSLVN'den 6'sı (%26,1) 1 cm'den büyüktü. Tüm RSLVN'ler T1W ve T2W'de izointens, FLAIR sekansında ise hiperintensti. DAG'de 23 RSLVN'den 20'sinde izointens sinyal vardı, geri kalan 3 lezyon ise hiperintens idi. Ortalama ADC değeri ve nADC oranı sırasıyla $1,42 \pm 0,29 \times 10^{-3} mm^2$ ve $1,87 \pm 0,31$ idi.

Sonuç: RSLVN sıklığı daha önce bildirilenden daha sık olabilir. Konvansiyonel MR görünümleri ve tipik lokalizasyonları ayırt edicidir ve nispeten büyük boyutlara ulaşabilirler. Takip sırasındaki morfolojik stabilite ve bu lezyonların ADC değerleri olası benign bir doğaya işaret etmektedir.

Anahtar Kelimeler: RSLVN, Nörogörüntüleme, Manyetik Rezonans Görüntüleme, Nodül, Lateral Ventrikül.

INTRODUCTION

Ring-shaped lateral ventricular nodules (RSLVNs) are rare lesions attached to the ependyma located in the body or roof of the lateral ventricles. They are generally considered to be a "leave me alone" lesion not associated with clinical symptoms. However, the exact nature of RSLVNs is unknown due to the lack of adequate histopathological data (1,2). Some previous reports have suggested that RSLVNs may be a precursor or variant of subependymoma (3,4).

Various typical imaging findings of RSLVNs have previously been described on conventional brain MRI, including T1W, T2W, FLAIR, and contrast-enhanced sequences (1,2). However, the extremely rare prevalence of these lesions raises the question of the reliability of the available data. Moreover, to our best knowledge, the apparent diffusion coefficient (ADC) values of these lesions on diffusion MRI have not been measured before (1,2,5). The aim of this study was to evaluate the conventional brain MRI findings of RSLVNs and to assess the ADC values of these lesions along with signal intensity characteristics in diffusion MRI.

MATERIAL AND METHODS

Ethics Approval: This retrospective study was approved by our institutional ethics committee (Decision number: 826153) and carried out according to the requirements of the Declaration of Helsinki. Informed consent was waived because of the retrospective nature of the study.

Patient Selection: The MR images of all patients who underwent contrast-enhanced cranial MRI in our institution between February 2019 and June 2023 were retrospectively evaluated. The exclusion criteria were: a) patients with cranial MRI examinations not suitable for evaluation due to motion or other artifacts; b) patients with collapsed lateral ventricles; c) known systemic or primary brain malignancy; d) history of brain radiotherapy or systemic chemotherapy.

MRI Protocol: MRI were performed using a 3 Tesla MR scanner (Ingenia; Philips Healthcare, Best, Netherlands). In all patients, the brain MRI protocol included the following sequences: sagittal turbo spin echo (TSE) T2, axial TSE T2 (repetition time (TR) 3,000 ms, echo time (TE) 80 ms, field-of-view (FOV) 185 mm × 230 mm, matrix size 400 × 320, slice thickness=5 mm), axial TSE T1 (TR 520 ms, TE 15 ms, FOV 256 mm × 256 mm, matrix size 400 × 320, slice thickness 5 mm), axial fluid attenuation inversion recovery (FLAIR) (TR 11,000 ms, TE 125 ms, inversion time 2500 ms, FOV 185 mm × 230 mm, matrix size 370 × 260, slice thickness=5 mm), axial single-shot echo-planar diffusion weighted imaging (DWI; TR 3200 ms, TE 80 ms, FOV 230 mm, matrix size 256 × 256, slice thickness = 5 mm, b value = 0-1000 mm^2/s) and pre- and post-contrast 3D T1 turbo fast echo (TFE) (TR/TE=26/6.2ms, FOV 24-26 cm, voxel size 1×1×1 mm^3, matrix=256 × 256, flip angle=25°). In addition, 3D Brain VIEW FLAIR sequence (TR 4800 ms, TE 351 ms, inversion time 1600 ms, FOV 20-24 cm, voxel size 1.5×1.5×1.5 mm^3, matrix size 216 × 180) was also available in some cases.

MRI Evaluation: MR images were reviewed by two experienced neuroradiologists (S.A and B.K., with 14 and 11 years of experience in neuroimaging, respectively) and any discrepancy resolved by consensus. MRI evaluation was performed using a dedicated PACS workstation (IntelliSpace Portal v7.0; Philips Healthcare, Best, Netherlands).

RSLVNs were diagnosed as ring-shaped nodular lesions attached to the lateral ventricular wall. Following the identification of each lesion, the number, location, shape and maximal axial diameter of the RSLVN were evaluated. In addition, the signal intensity of the ring portion of the nodules was assessed relative to the surrounding white matter, and the signal intensity of the core portion was assessed relative to the cerebrospinal fluid (CSF) on T1W, T2W and FLAIR images. Contrast enhancement characteristics of lesions were also evaluated.

On DWI, firstly, whether the RSLVN has diffusion restriction and its signal intensity characteristics (b1000) were visually evaluated. The ADC value was measured by placing a free-hand region of interest (ROI) of 5-40 mm^2 area in the ring portion of the lesion, avoiding the central core portion. Furthermore, normalized ADC (nADC) ratios are calculated as the ratio of the ADC in the tumor to the ADC in normal appearing contralateral white matter.
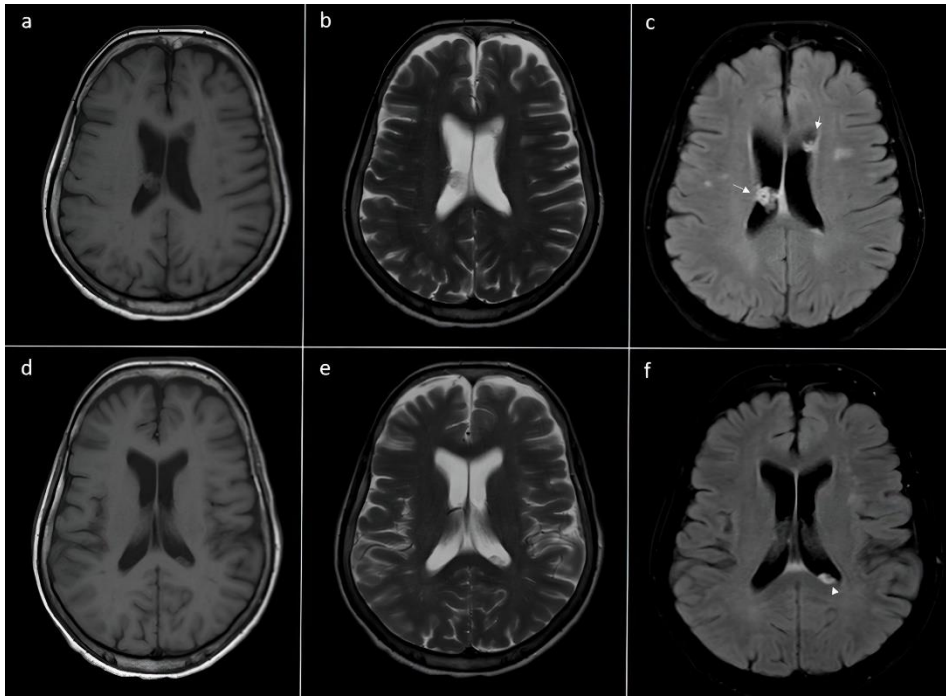
If follow-up MRI examinations were obtained, morphological changes of RLSVNs over time were evaluated.

Statistical Analysis: Statistical analyses were performed using SPSS version 21.0 software (SPSS Inc., Chicago IL, USA). Percentages (%) were used for categorical data and median values were used for continuous data in descriptive statistics.

RESULTS

A total of 2920 brain MRI examinations were evaluated and RSLVN was detected in 15 patients (0.51%). The mean age of 15 patients with RSLVN was 53.6 ± 16.07 (range 28-81) and 73.3% (n=11) of them were female. Brain MRI indications were headache in six patients, vertigo in two patients, screening for trauma in two patients, hemifacial spasm in one patient, meningioma follow-up in one patient, confusion in one patient, ICA aneurysm in one patient, and vertebral artery dissection in one patient.
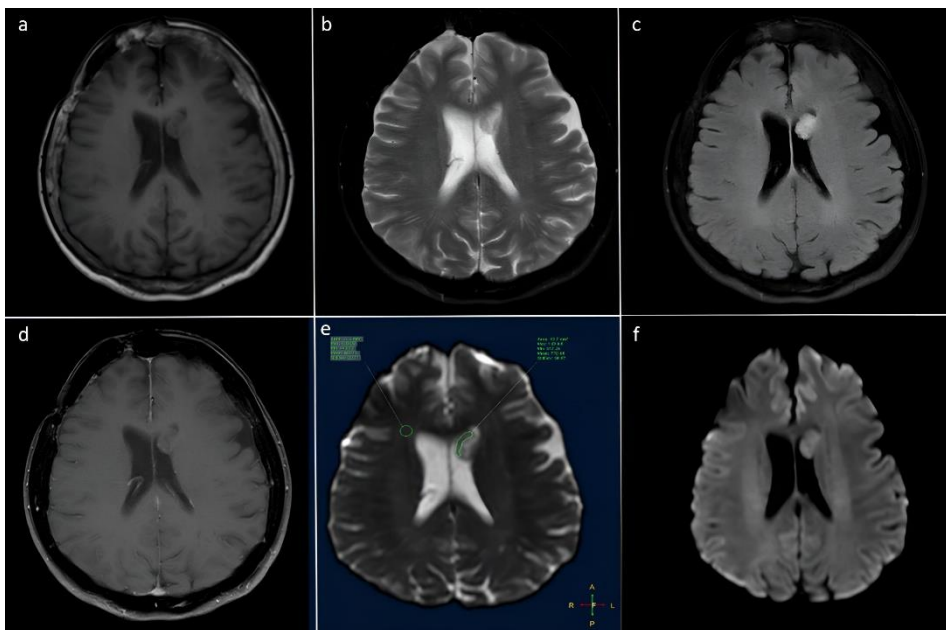
Ten patients had a single RSLVN, while three patients had three and two patients had two.
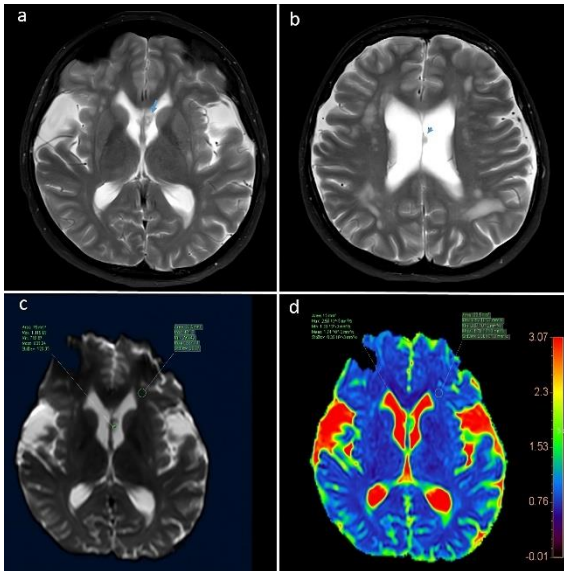
Figure 1. Three RSLVNs in different locations in a 71-year-old female patient (case 10). T1W (**a**), T2W (**b**) and FLAIR (**c**) images show two RSLVNs located in the body of the right lateral ventricle and the frontal horn of the left lateral ventricle, measuring 13mm and 9mm, respectively. In addition, T1W (**a**), T2W (**b**) and FLAIR (**c**) images of more inferior sections show another RSLVN in the left lateral ventricle. All identified RSLVNs have isointense signal on T1W and T2W and hyperintense signal on FLAIR

Therefore, a total of 23 RSLVNs were identified in fifteen patients. Nodules were located on the roof of the lateral ventricle body in eight nodules (34,8%), in the frontal horn in twelve nodules (52.2%), and in the septum pellucidum in three nodules (13%) (Figure 1). The mean maximum diameter of the RSLVNs was 7.73 mm (range 2-15 mm) and six nodules (26.1%) were larger than 1 cm. Of the 23 RSLVNs, 9 were lobular in shape, 8 were round, and 6 were oval.

Figure 2. MRI findings of RSLVN located in the left frontal horn in a 63-year-old female patient (case 14). The peripheral portion of the lesion has hypointense signal on T1W (**a**) and T2W (**b**), hyperintense signal on FLAIR (**c**), and does not show enhancement on contrast-enhanced T1W image (**d**). On the other hand, the central portion of the lesion has the same intensity as the CSF on all sequences. **e** Measurement of ADC values of RSLVN and contralateral normal-appearing white matter is performed on grey-scale ADC images. **f** The lesion is slightly hyperintense on DWI (b1000)**.** This patient had previously undergone surgery due to sphenoid wing meningioma

Figure 3. RSLVNs located in the septum pellicidum (case 8). **a,b** Axial T2-weighted images show two RSLVNs, 12 mm and 2 mm in size respectively, located in the septum pellicidum. **c,d** b0 DWI image and color ADC map of the 12 mm sized RSLVN, which is located more inferiorly. The mean ADC value of the lesion was measured as $1.74 \times 10^{-3} mm^2$

In all of the 23 RSLVNs, the signal intensity of the ring portion relative to the surrounding white matter, and the signal intensity of the core portion relative to CSF was isointense on T1- and T2-weighted imaging. On FLAIR imaging, all RSLVNs showed hyperintense signal. Contrast enhancement was not observed in any of the lesions on post-contrast T1-weighted imaging. On DWI, none of RSLVNs showed true diffusion restriction. 20 of 23 RSLVNs had isointense signal on DWI (b1000) compared to the adjacent brain parenchyma. On the other hand, the remaining 3 lesions were hyperintense on DWI (b1000) (Figure 2). The mean ADC of the 15 evaluated RSLVNs was $1.42 \pm 0.29 \times 10^{-3}$ mm^2/s, while the mean nADC ratio was 1.87 ± 0.31 (Figure 3).

No morphological changes were observed in any of the 16 RSLVNs in 12 patients with follow-up MRI at a median of 16.5 months. Detailed clinical and radiological findings are shown in Table 1.

DISCUSSION

In this study, we report the MRI and clinical findings of RSLVN in the largest population to date. Our study reveals that RSLVN is more common than previously reported. Shimono et al. reported the prevalence of RSLVN as 0.023%, while Nakajima et al. reported it as 0.45% (1,2). The higher prevalence in our study may be due to the higher awareness of RSLVN thanks to previous reports and the inclusion of lesions >1 cm. Various studies on RSLVNs have described them as nodular lesions commonly smaller than 1 cm (1,2,5,6). On

the other hand, Pontillo et al. reported a giant RSLVN larger than 2.5 cm causing a mass effect and showed that these ring-shaped lesions can reach large sizes (3). In our study, six RSLVNs larger than 1 cm were observed, the largest of which was 15 mm in size.

Most of the cases diagnosed with RSLVN in the literature are middle-aged or older individuals, and it has been observed more frequently in male patients (1-6). In our study, RSLVN was also detected in middle-aged and older adults. However, most of our patients with RSLVN were female patients (73.3%). The roof of the body of the lateral ventricle or the frontal horn are reported as the typical locations of RSVLNs, as in most lesions in our study (1,2). On the other hand, for the first time, we observed RSLVNs located in the septum pellicidum in a patient.

The characteristic appearance of RSLVNs on conventional MR imaging is that the peripheral ring portion is isointense on T1W and T2W compared to the brain parenchyma and does not show contrast enhancement. On FLAIR imaging, although Shimono et al. identified two exceptionally isointense RSLVNs, the hyperintense signal is distinctive. In addition, the core portion of the RSLVN is expected to be isointense to CSF on T1WI, T2WI and FLAIR (1,2,5). Conventional MRI findings in our study confirmed these characteristic MRI features.

Previous studies and case reports have revealed that RSVLNs do not show diffusion restriction and have an isointense signal relative to the surrounding brain parenchyma on DWI (1-3). In our study, none of the RSLVNs showed diffusion restriction and the vast majority of them were isointense on DWI. However, unlike previous studies, 13% (n = 3) of the RLSVNs had hyperintense signal on DWI. In addition, we measured the ADC values (absolute ADC and nADC ratio) of RSLVNs for the first time. These ADC values of RSLVNs can provide information about the possible nature of these nodules and serve as a reference for future studies. ADC values are a major determinant of tumor cellularity in brain tumors, and high ADC values are associated with low cellularity. For gliomas and meningiomas, absolute ADC values above $0.8-1 \times 10^{-3}$ mm^2/s generally indicate low cellularity and low-grade tumor (7,8). Moreover, since the absolute ADC values in benign tumors are usually higher than the normal-appearing white matter, the nADC ratios in these tumors are above 0.99 (9). Therefore, the high ADC values and nADC ratios of RSLVNs in our study support that these lesions are probably of a benign nature.

Although the exact nature of RSLVNs is unknown due to inadequate histopathological data, five different possibilities have been hypothesized: a) neuroglial or glioependymal cyst; (b) inflammatory nodular formation of ependyma

Table 1. Magnetic resonance imaging and clinical features of patients diagnosed with RSLVN

Case	Age/Sex	Location	Shape /Diameter	Signal intensity on T1WI	Signal intensity on T2WI	Signal intensity on FLAIR	Signal intensity on DWI	ADC value	NADC ratio	Contrast enhancement	Follow-up period
1	38/M	Right frontal horn	Oval/4 mm	Isointense	Isointense	Hyperintense	Isointense	1.22	1.67	None	N/A
		Left frontal horn	Round/3mm	Isointense	Isointense	Hyperintense	Isointense	N/A	N/A	None	
		Roof of left body	Round/3mm	Isointense	Isointense	Hyperintense	Isointense	N/A	N/A	None	
2	46/F	Right frontal horn	Oval/ 11mm	Isointense	Isointense	Hyperintense	Isointense	1.02	1.54	None	4 months
3	43/F	Right frontal horn	Lobular/14mm	Isointense	Isointense	Hyperintense	Isointense	1.42	1.91	None	8 months
4	76/F	Roof of left body	Round/5mm	Isointense	Isointense	Hyperintense	Isointense	1.46	1.71	None	50 months
		Right frontal horn	Round/4mm	Isointense	Isointense	Hyperintense	Isointense	N/A	N/A	None	
5	81/F	Roof of right body	Lobular/ 9mm	Isointense	Isointense	Hyperintense	Isointense	1.75	2.36	None	37 months
6	40/F	Roof of right body	Lobular/ 9mm	Isointense	Isointense	Hyperintense	Isointense	1.20	1.73	None	5 months
7	66/M	Right frontal horn	Oval/ 6mm	Isointense	Isointense	Hyperintense	Isointense	1.98	2.4	None	5 months
8	28/F	Septum pellucidum	Oval/12mm	Isointense	Isointense	Hyperintense	Isointense	1.81	2.38	None	N/A
		Septum pellucidum	Round/3mm	Isointense	Isointense	Hyperintense	Isointense	N/A	N/A	None	
		Septum pellucidum	Round/2mm	Isointense	Isointense	Hyperintense	Isointense	N/A	N/A	None	
9	51/M	Roof of left body	Round/ 5mm	Isointense	Isointense	Hyperintense	Isointense	1.21	1.77	None	N/A
10	71/F	Roof right body	Lobular/13mm	Isointense	Isointense	Hyperintense	Isointense	1.80	2.19	None	12 months
		Left frontal horn	Lobular/ 9mm	Isointense	Isointense	Hyperintense	Isointense	N/A	N/A	None	
		Roof of left body	Lobular/ 7mm	Isointense	Isointense	Hyperintense	Isointense	N/A	N/A	None	
11	41/F	Right frontal horn	Lobular/11mm	Isointense	Isointense	Hyperintense	Hyper-intense	1.56	1.91	None	16 months
12	56/M	Left frontal horn	Lobular/11mm	Isointense	Isointense	Hyperintense	Isointense	1.55	2,03	None	18 months
13	70/F	Right frontal horn	Oval/ 8mm	Isointense	Isointense	Hyperintense	Isointense	1.12	1.47	None	52 months
		Left frontal horn	Round/5mm	Isointense	Isointense	Hyperintense	Isointense	N/A	N/A	None	
14	63/F	Left frontal horn	Lobular/15mm	Isointense	Isointense	Hyperintense	Hyper-intense	1.24	1.58	None	17 months
15	34/F	Roof of left body	Oval/9mm	Isointense	Isointense	Hyperintense	Hyper-intense	1.1	1.54	None	24 months

similar to granuloma; (c) astrocytic gliosis reactive to adjacent subependymal veins; (d) redetachment of the fused portion of coarctation of the ventricle frontal horns; (e) variety of subependymoma (1). The most prominent among these is subependymoma. Because two recent reports revealed the histopathological diagnosis of RLSVNs as subpendymoma (3,4). Moreover, subependymomas located in the lateral ventricle may have various clinical and radiological features resembling RSLVNs. Subependymomas are intraventricular, usually smaller than 2 cm, lobular, well-circumscribed, non-enhancing tumors on MRI, which are usually detected incidentally in middle-aged and elderly adults (10,11). They may be localized in the body of the lateral ventricle, the frontal horn, or the septum pellucidum and have a ring-shaped appearance (3,12). These features are also commonly observed in RSLVNs in the literature and in our study (1,2,6). Additionally, subependymomas can be multiple, like RSLVNs (11).

The morphological stability of RSLVNs over time and their lack of association with clinical symptoms emphasize the possible benign nature of these lesions. Thus, the optimal management recommended for RSLVNs with typical clinical and radiological features is periodic follow-up (5).

Limitations: The main limitations of our study were the retrospective design and relatively small sample size. In addition, ADC measurements was not performed in some lesions due to small lesion size. Finally, none of the identified RSLVNs had a histopathological diagnosis.

CONCLUSION

Our study is the largest experience reported in the literature to date regarding the MRI and clinical characteristics of RSLVNs. These lesions may be more common than previously reported and can reach sizes greater than 1 cm. Their distinctive MRI appearances and typical localizations (body of the lateral ventricle, frontal horn and septum pellucidum) are helpful in making the diagnosis. The absence of association with symptoms, morphological stability during the follow-up interval and high ADC values suggest a possible benign nature.

Declarations:

Funding: No funding was received for conducting this study.

Compliance with Ethical Standards

Ethics approval: This study was performed in line with the principles of the Declaration of Helsinki. Approval was granted by the Ethics Committee of Istanbul University-Cerrahpasa.

Conflicts of Interest: The authors have no relevant financial or non-financial interests to disclose.

Informed Consent: Informed consent was waived because of the retrospective nature of the study.

REFERENCES

1. Shimono T, Hosono M, Ashikaga R, Kumano S, Imaoka I, Yagyu Y, et al. Ring-shaped lateral ventricular nodules: an incidental finding on brain magnetic resonance imaging. Neuroradiology. 2009;51(3):145-50.
2. Nakajima R, Uchino A, Saito N, Nishikawa R. Ring-shaped Lateral Ventricular Nodules Detected with Brain MR Imaging. Magn Reson Med Sci. 2013;12 (2):105-10.
3. Pontillo G, Lepore G, Bartolini A, Cerase A, Brunetti A, Muccio CF. Is This Truly A "Leave-Me-Alone" Lesion? An Unusual Case of Multiple Ring-shaped Lateral Ventricular Nodules. World Neurosurg. 2020;136:32-6.
4. Kuya K, Shinohara Y, Yoshioka H, Kuwamoto S, Kurosaki M, Ogawa T. A Case of Intracranial Subependymoma: Histopathological Confirmation of Ring-shaped Lateral Ventricular Nodule. Magn Reson Med Sci. 2018;17(2):105-6.
5. Romano N, Fiannacca M, Castaldi A. Imaging of ring-shaped lateral ventricular nodules (RSLVNs). Neurol Sci. 2023;44(6):2223-5.
6. Rosa Júnior M, Vieira VLF. Ring-shaped lateral ventricular nodules: a "leave me alone" lesion. Arq Neuropsiquiatr. 2018;76 (7):494.
7. Kono K, Inoue Y, Nakayama K, Shakudo M, Morino M, Ohata K, et al. The Role of Diffusion-weighted Imaging in Patients with Brain Tumors. Am J Neuroradiol. 2001;22 (6):1081-8.
8. Wang Q, Zhang J, Xu X, Chen X, Xu B. Diagnostic performance of apparent diffusion coefficient parameters for glioma grading. J Neurooncol. 2018;139(1):61-8.
9. Nagar VA, Ye JR, Ng WH, Chan YH, Hui F, Lee CK, et al. Diffusion-Weighted MR Imaging: Diagnosing Atypical or Malignant Meningiomas and Detecting Tumor Dedifferentiation. Am J Neuroradiol. 2008;29(6):1147-52.
10. Hoeffel C, Boukobza M, Polivka M, Lot, G, Guichard, JP, Lafitte F, et al. MR manifestations of subependymomas. AJNR Am J Neuroradiol. 1995;16(10):2121-9.
11. Bi Z, Ren X, Zhang J, Jia W. Clinical, radiological, and pathological features in 43 cases of intracranial subependymoma. J Neurosurg. 2015;122(1):49-60.
12. Nishio S, Morioka T, Mihara F, Fukui M. Subependymoma of the lateral ventricles. Neurosurg Rev. 2000;23(2):98-103.